Skeletons:
Application & Construction

Prof. Deborah Silver
Dept. of Electrical and Computer Engineering

Grad Students: *Nicu Cornea, Jian Chen, Jamshed Datsur, Lian Jiang, Kristina Santilli, Vikas Singh,*

Visualization & Graphics

November 2003

http://www.caip.rutgers.edu/vizlab.html

Outline

•Skeleton Definition
•Skeleton Application
•Skeleton Construction : Survey
•Extra

Curve-Skeleton in 3D

- 3D polygonal datasets
- 3D volumetric dataset
- 3D point sample

3D Model: Volumetric Dataset

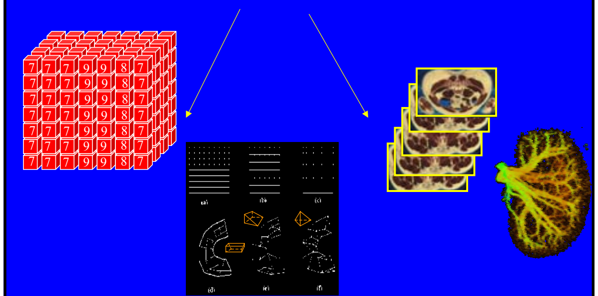

Types of Grids

3D Model: Polygonal Dataset

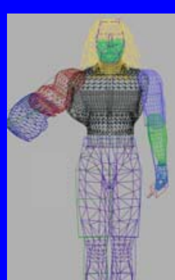

3D Model: scattered point samples

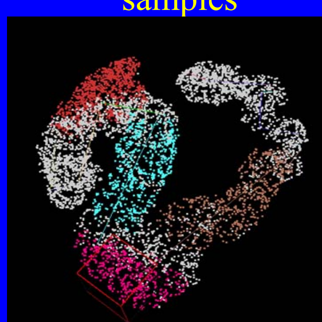

What is a skeleton?

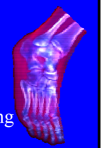

Webster ---

- 1. (a) a hard internal or external framework of bones, cartilage, shell, woody fibre, etc., supporting or containing the body of an animal or plant. (b) the dried bones of a human being or other animal fastened together in the same relative positions as in life.
- 2. the supporting framework or structure or essential part of a thing.
- 3. a very thin or emaciated person or animal.
- 4. the remaining part of anything after its life or usefulness is gone.
- 5. an outline sketch, an epitome or abstract.
- 6. ("attrib.") having only the essential or minimum number of persons, parts, etc. ("skeleton plan"; "skeleton staff").

What is a skeleton?

- Locus of centers of maximal 2D Disks or 3D Balls contained within an object
- Meeting of wavefronts initiated at the object boundary --- grassfire analogy.
  - 2D --- Medial Axis
  - 3D --- Medial Surface
  - **3D --- Curve-skeleton, centerline, line-skeleton,**

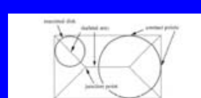

H. Blum, A Transformation for Extraction New Descriptors of Shape, Models for the Perception of Speech and Visual Form, MIT Press, 1967.

Examples of Curve-Skeletons

What it is --- depends upon the application it is being used for.

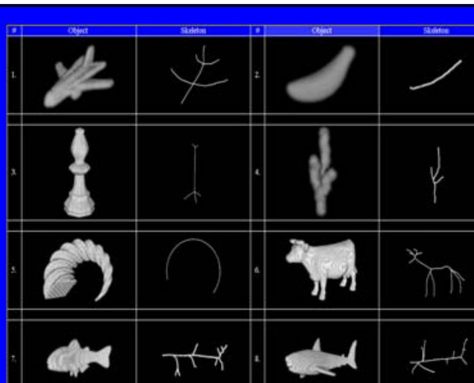

Curve-Skeleton examples

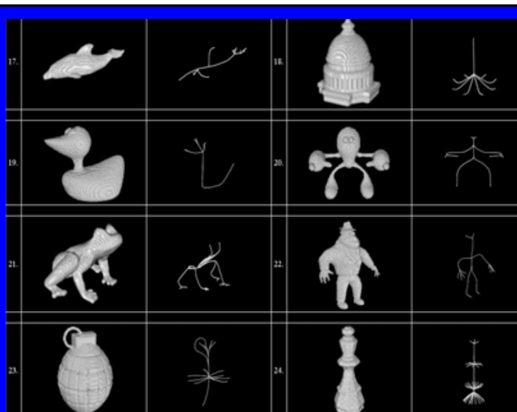

More curve skeleton examples

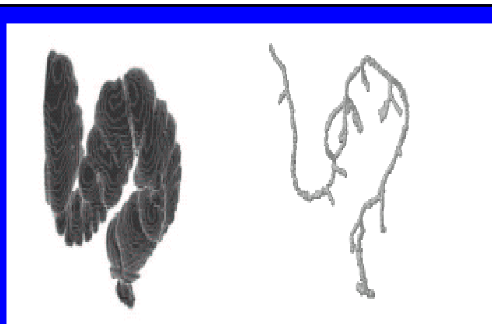

The colon data set and the corresponding skeleton

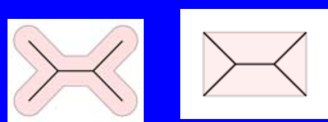

The same skeleton may belong to different objects

Desirable Properties of 3D Curve-Skeletons

- **Thinned** representation of an object – ideally 1-voxel thick for curve-skeletons
- Captures the "shape" of the object (**Homotopy**)
- "**Centered**" within the object – locally centered with respect to the objects boundary
- **Connectedness**: A set of connected voxels
- **Robustness**: Insensitive to small perturbations/noise on the boundary or rotation of the object
- **Efficiency**: Should be efficient to compute
- **Reconstructability**: Can reconstruct the 3D object from its skeleton
- **Reliability/Visibility**: Every interior boundary point should be visible from the skeleton (visibility coverage)
- **Component based**: different segments of the skeleton are distinguishable
- **Hierarchical/Level-of-Detail**: Different hierarchies of skeleton complexity are computable
- **Symmetry** ---- If the object is symmetric the skeleton should also be symmetric.

Properties of Curve-skeletons

- Based upon the application
- Some of the properties are conflicting (thinness vs. reconstructability)

Volume Reconstruction

- Distance Transform (min. distance to the boundary) is stored at every skeleton voxel.
- A sphere centered at a skeleton voxel of radius equal to the distance transform is tangential to the boundary.

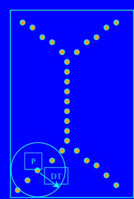

Reconstruction

- Filling in the spheres centered at skeleton voxels reconstructs the object.
- Reconstruction quality depends on the number of skeleton voxels

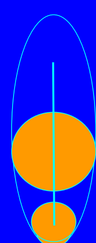

Hierarchical/Level-of-Detail

Example Skeletonizations

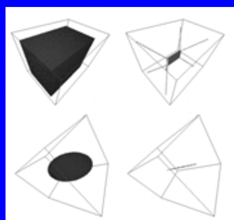

Cuboids and obloids have a very well defined skeleton that allows lossless reconstruction

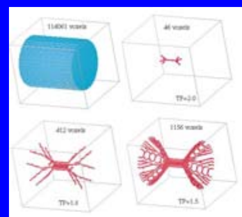

Other shapes - such as cylinders, and most irregular objects - produce skeletons with varying degree of loss.

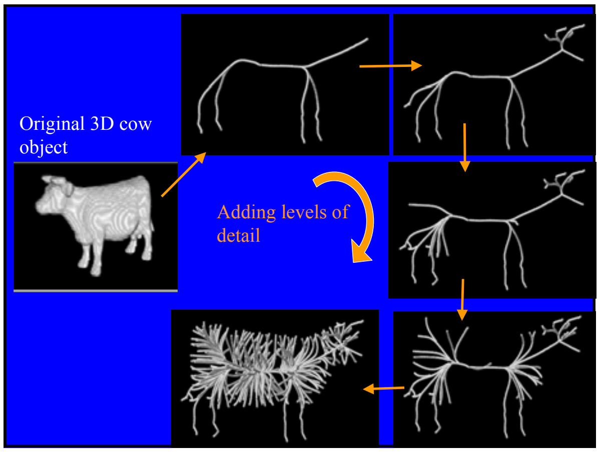

Not necessarily unique

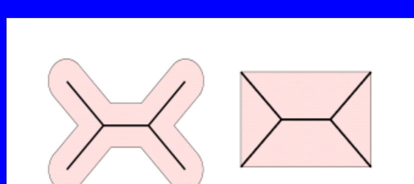

Applications of Skeletonization

- Improved/Alternate visualization
- Quantification/Measurements

Applications…..

Non Photorealistic Rendering (NPR)

….in the "Artistically Challenged" style

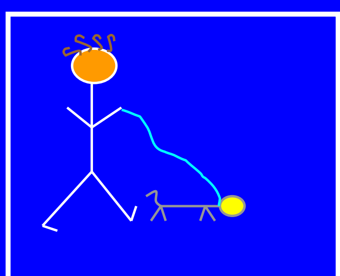

Seriously…

- Skeletons are simplified abstractions or "figural models" which can help explain the shape of 3D objects.

Virtual Navigation

- Virtual Endoscopy/Colonoscopy
- Steps:
  - MRI/CT of organ
  - Get Centerline
  - Position virtual camera along centerline
    →thinness, centrality, efficiency & visibility important

Y. Zhou, A. Kaufman and A.W Toga, ***Three-dimensional Skeleton and Centerline Generation Based on an Approximate Minimum Distance Field***, The Visual Computer, vol. 14, pp. 303-314, 1998.

T. He, L. Hong, D. Chen and Z. Liang, ***Reliable Path for Virtual Endoscopy: Ensuring Complete Examination of Human Organs***, IEEE Trans. Visualization and Computer Graphics, vol-7, no. 4, pp. 333-342, 2001.

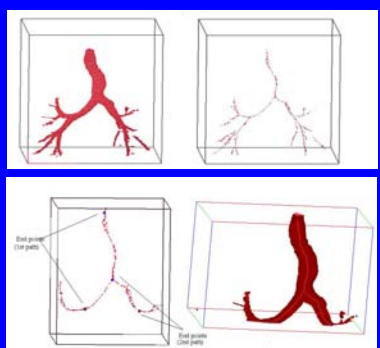

Generating centerlines for automatic navigation using skeletons. Shown here is the human trachea dataset.

Using a Skeleton-Centerline for automatic navigation: *virtual camera flythroughs*

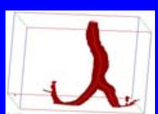

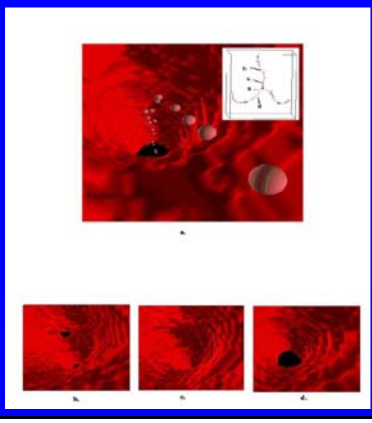

Skeleton based Animation

- IK skeleton used for animation in computer graphics

Example: Standard Character Animation

- Create a polygonal model
- Create a Skeleton to fit that polygonal model (done by an animator). The skeleton is a thin ball and stick abstraction of the model.
- Bind the polygons in the model to joints in the skeleton.
- Deform the skeleton to cause a corresponding deformation in the model using key-framing, inverse kinematics and motion capture

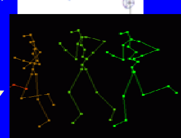

Screen Snapshot from Character Studio

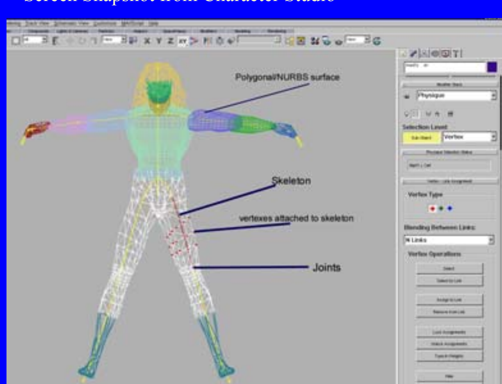

Goal: Automatically compute IK skeleton & bindings

Hierarchical Mesh Decomposition using Fuzzy Clustering and Cuts
By Tal and Katz, Siggraph 2003.

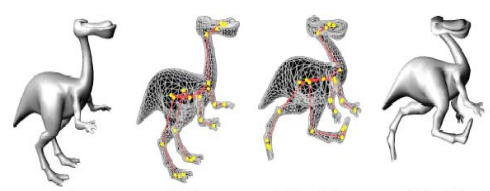

(a) object (b) skeleton (c) deformed skeleton (d) deformed object

Figure 2: Deformation of a dino-pet

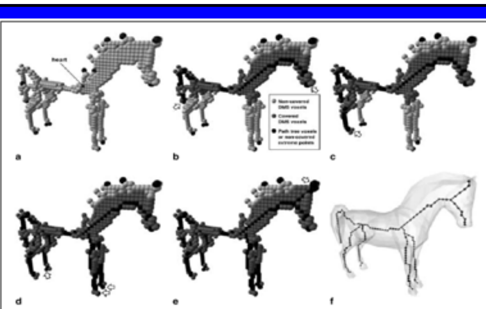

Fig. 3a–f. Forming path-tree extension. **a** DMS of a horse with the heart voxel labeled and the extreme points drawn as *black spheres*. The extreme point at the tip of the tail is the first point of the path tree. **b** The first extension to the path tree reaches from the tail to the nose. **c** The second extension reaches to the right hind hoof. **d** The next three extensions branch out to the other hooves. **e** The final branch extends to the ears. The remaining extreme points are not far enough from the covered region to warrant further extensions of the path tree. **f** The completed path tree without the other DMS voxels; path-tree voxels are drawn as *small spheres* to allow the edges of the path tree to be seen

Automated Generation of Control Skeletons for Use in Animation
L. Wade and R. Parent, The Visual Computer, 18(2), March 2002.

Volume animation using skeleton tree

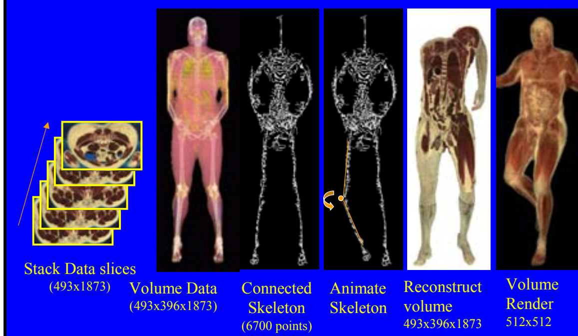

Animation of the Visible Human

- Articulated skeleton, sampled reconstruction
- Animated using motion capture data in Character Studio.
- Each frame is a 3D dataset

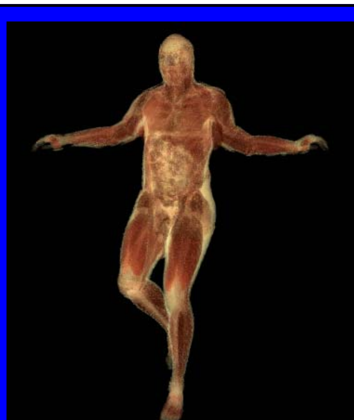

Skeletons for Volume Manipulation

Moving occluding parts from a volume

Volumetric Monkey

Original

Deformed – Bent leg

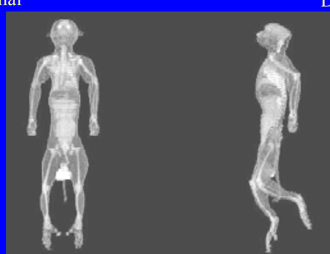

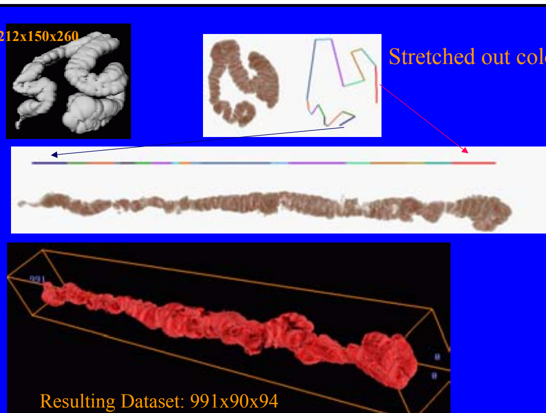

Stretched out colon

Slicing the stretched colon

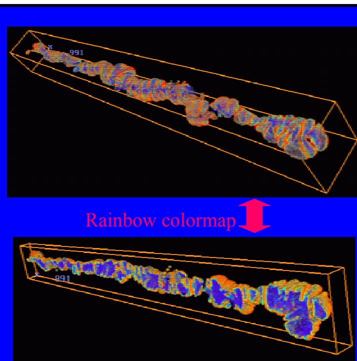

Using a Medial Surface for Animation

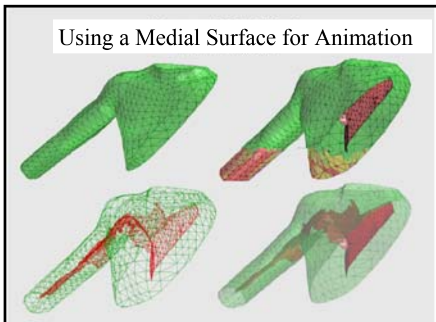

J. Bloomenthal, Model based Vertex Deformation, *Symposium On Computer Animation,* 2002.

Vertex deformation is a popular technique to animate an erstwhile static object. It is difficult, however, to deform those vertices near multiple limbs of the controlling stick-figure skeleton while maintaining a natural-appearing surface. By applying convolution to the medial axis/surface of the object, the weights associated with vertex deformation can be computed automatically. Fewer undesire artifacts are evidenced in the animated surface

Skeletons for Collision Detection

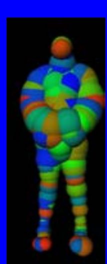

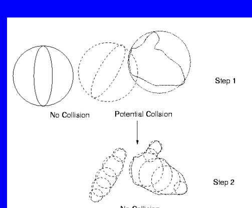

Curved Planar Reformation

- Medial-axis reformation: curved sections of branched vessels are displayed on one image – cut throughs can also be shown to display diameter --- CT Angiography (pulmonary embolism and aortic dissection)

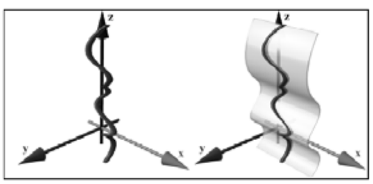

Figure 3.7: Left: A curved spatial line. Right: A curved plane defined by the curved line and a vector parallel to the x-axis.

The process of extracting a set of voxels lying on the curved plane and displaying this set as a straightened plane is called *curved planar reformation*. This process distorts the resulting image in terms of distances and anatomic relationships. However, this visualization technique resolves the problem of overlapping (i.e., occluding) objects. Another advantage of this visualization method is that artery diseases can be seen very fast.

Visualization of tubular structures such as blood vessels is an important topic in medical imaging. One way to display tubular structures for diagnostic purposes is to generate longitudinal crosssections in order to show their lumen, wall, and surrounding tissue in a curved plane. Vascular abnormalities (i.e., stenoses, occlusions, aneurysms and vessel wall calcifications) are then investigated by physicians. This process is called Curved Planar Reformation (CPR) or Multi Planar Reformation (MPR).

CPR - Curved Planar Reformation
Armin Kanitsar¤ Dominik Fleischmann† Rainer Wegenkittl‡ Petr Felkel‡ Meister Eduard Gr¨oller
IEEE Visualization 2002, 2003

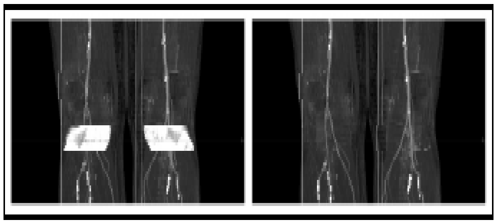

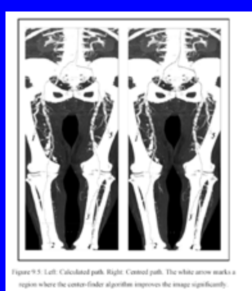

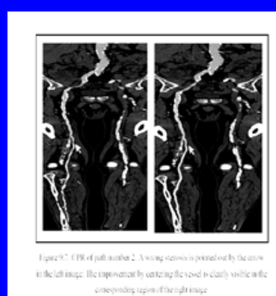

Advanced Visualization Techniques for Vessel Investigation}, school = {University of Technology Vienna, Institute of Computergraphics and Algorithm}, month = mar, year = 2001, url = {http://www.cg.tuwien.ac.at/research/vis/angiovis/}

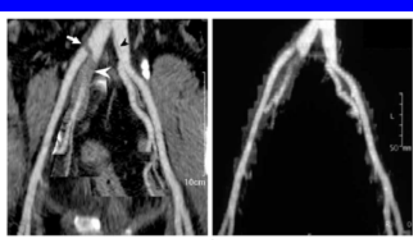

a. b.

Figure 7. Case 4. (a) Electron-beam CT angiogram reconstructed with MAR shows aortic dissection involving the left common iliac artery (black arrowhead), right common iliac artery (arrow), and right internal iliac artery (white arrowhead). Vessels were spread to their full length. (b) Image reconstructed with MIP does not display the flap in the left common iliac artery clearly. The internal iliac arteries were shortened because of the projection.

Medial Axis Reformation:
A New Visualization Method for CT Angiography[1]

Sha He, MS, Ruping Dai, MD, Bin Lu, MD, PhD, Cheng Gao, MD, Hua Bai, BS, Baolian Jing, MD

Figure 1: An untangled vascular tree of the peripheral arteries.

A. Kanitsar, R. Wegenkitt, D. Fleischmann and M. Groller, ***Advanced Curved Planar Reformation: Flattening of Vascular Structures,*** Vis. 2003

Vessel Tracking

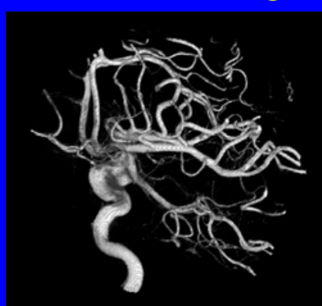

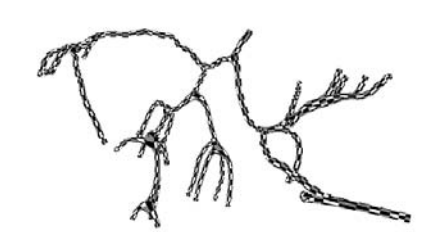

Figure 9: Example of a liver vessel tree surface (for better clearness with differently colored patches and a constant radius)

SMART-Surface models from by-axis-and-radius-defined tubes (2002) Petr Felkel, Armin Kanitsar, Anton L. Fuhrmann, Rainer Wegenkittl

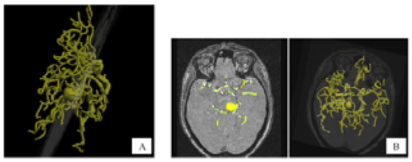

Figure 15. (A) Surface rendering of tubular representations extracted from an MRA of a patient with an arterio venous malformation; interested translucently into the 3D visualizations is a slice from the MRA volume. (B) Same patient's data: the left-hand image illustrates another slice of the MRA and its intersection with the extracted vessels is overlaid. The right-hand image is a 3D rendering from a different point of view that clearly illustrates the Circle of Willis and an aneurysm.

Measurements

- Measurements along the skeleton (length)
- Measurement of Core strength: Vortex Cores, Plume Cores

Hydrothermal Plume Simulation

Plume Accoustic Dataset

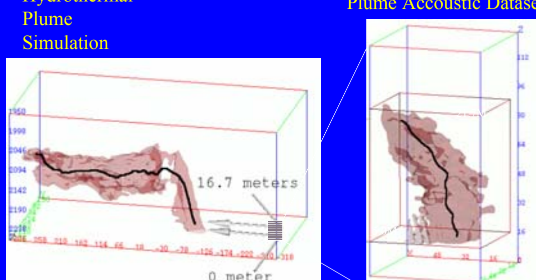

Simulation by: J. W. Lavelle and M. Wetzler, NOAA.

Dataset: P. Rona and K. Bemis

Protein Analysis

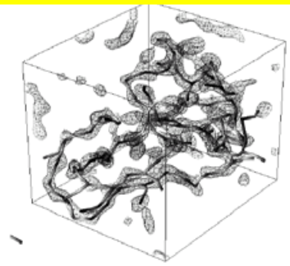

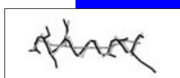

Figure 7: 3D contour and critical point graph for a unit cell of protein 4PTI (58 residues) constructed at 3 Å resolution. The critical point graph in this figure was generated using the output of the ORCRIT program.

L. Leherte and Janice I. Glasgow and Kim Baxter and E. Steeg and S. Fortier, Analysis of Three-Dimensional Protein Images, Journal of Artificial Intelligence Research, 7, 1997.

Feature Tracking

Automatically correlate extracted regions from one dataset to the next

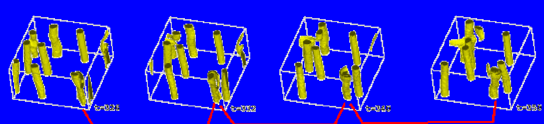

Assumption:
Sufficient Sampling Frequency such that corresponding features overlap in space.

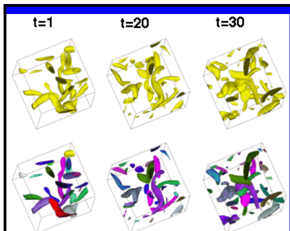

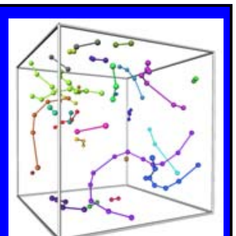

•Freek Reinders, Frits H. Post, and Hans J.W. Spoelder, "Visualization of Time-Dependent Data using Feature Tracking and Event Detection", *The Visual Computer*, Vol. 17, Nr. 1, pages 55-71, 2001.
Freek Reinders, Melvin E.D. Jacobson, and Frits H. Post, "Skeleton Graph Generation for Feature Shape Description", in *Data Visualization 2000*, W. de Leeuw, and R. van Liere (eds.), Springer Verlag, pages 73-82, 2000.

Shape Matching

- Fundamental problem of computer vision
- Various research areas
  - 3d Object Matching
  - Volumetric Matching
  - 3d image Registration
- Different Approaches
  - Image Based
    - Image Statistics, Harmonics etc …
  - Feature Based
    - Skeletons, Medial-axes, shape primitives

What is a good match ?

- The definition of a match between two objects is not clearly defined
  - Are these two objects similar ?

  - Are these two objects similar ?

- Need the matching to be controllable

Skeleton Matching

- Skeleton based
  - Generate a centerline representation of the Volumetric object
  - Generate a shape-graph from this centerline representation
  - Perform isomorphic subgraph matching on the graph obtained to other graphs present in the database
  - The graph nodes contain information about the local shape characteristics whereas the graph edges describe the global *shape* of the object. The matching parameters can be adjusted based on the kind of matching required.

Shape Matching

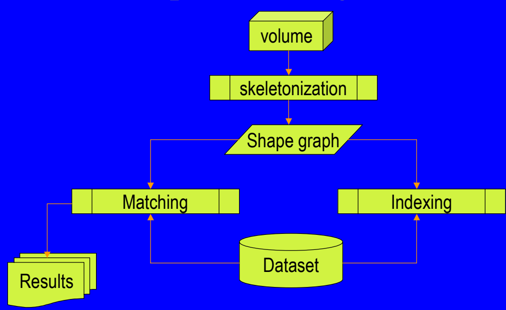

Matching the Shape Graphs

- At each node in the graph, a structural ``signature" is defined, which characterizes the node's underlying subgraph structure. This signature is a low-dimensional vector whose components are based on the eigenvalues of the subgraph's adjacency matrix.
- Each node also contains local shape information, which is the skeletal cloud attached to that node.
- Recursively find matches between vertices.
- Start at the root of the shape graph and proceed down through the subtrees in a depth-first fashion.
- Output a match metric that quantizes the match and also a list of matched nodes.

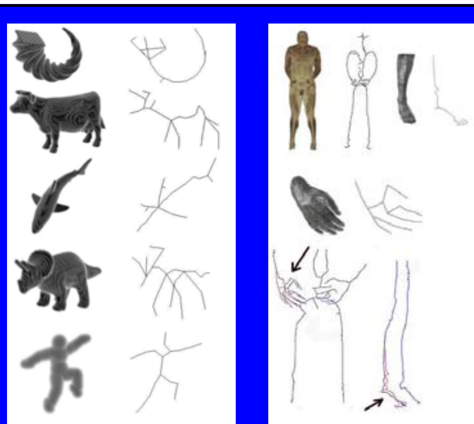

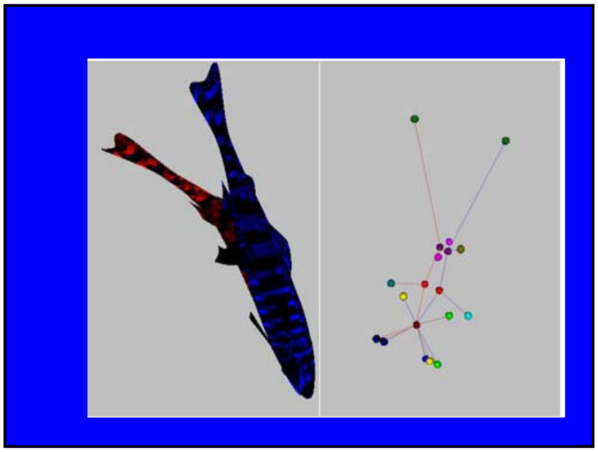

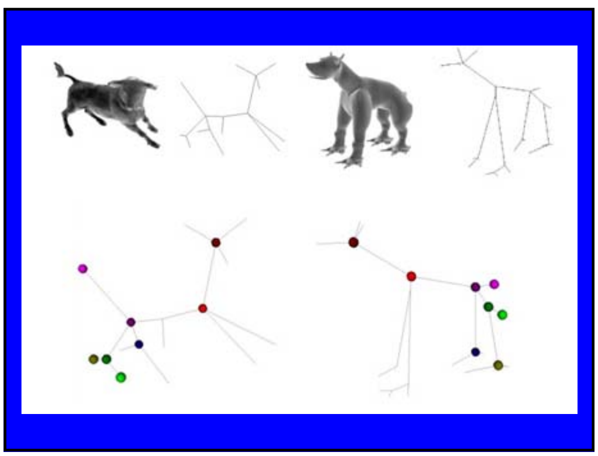

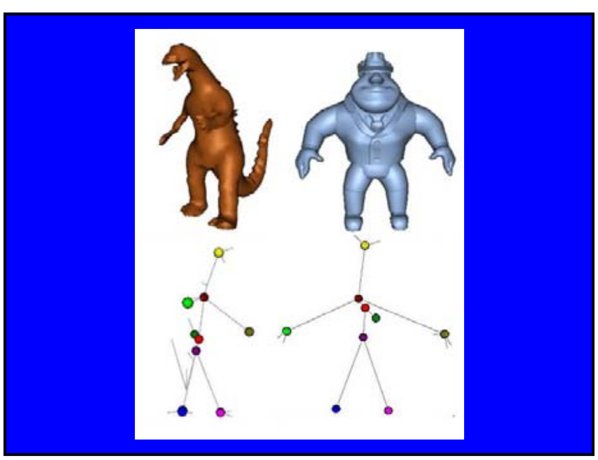

Feature based morphing

- Use skeleton to help morph objects → feature based
- Can do match & morph for better visualization

Skeleton-based three-dimensional geometric morphing
Robert L. Blanding, George M. Turkiyyah, Duane W. Storti and Mark A. Ganter. Computational Geometry, 15 (1-3), February 2000.

3D Registration

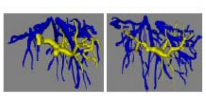

Fig. 4. Liver030(left) and Liver032(right) issued both from normal subjects. The hepatic system appears in dark and the portal in bright. The vasculatures differentiate a lot by the number and the location of the vessels

Vascular Atlas Formation
Using a Vessel-to-Image
Affine Registration Method

Dini Chillet, Julien Jomier, Derek Cool, and Stephen R. Aylward

MICCAI 03

Mesh Reconstruction

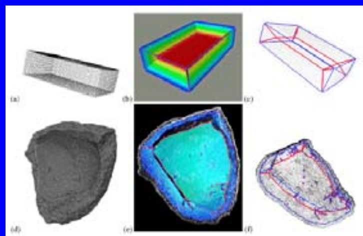

Figure 1.4: The shock scaffold of a rectangular box sampled by 7326 points (a) is depicted in (b) and (c). The flow along sheets is shown using the color spectrum, where blue means close to the boundary, and red means as far as possible. In (c) the geometry for the interior of the shock sheets is left implicit, and axial curves at the intercepts of shock sheets are shown in pink, while ridge curves at the boundaries of shock sheets are shown in blue. This synthetic example serves as a prototype of many real shapes, such as the pot sherd in (d) which can be thought of as a deformed rectangular box with additional surface perturbations (approximatively 40 000 point samples here). The shock scaffold of this sherd is shown in (e) with the flow along sheets color-coded similarly to (b) where the missing colors of the spectrum correspond to the symmetries away from the concave part of the pot sherd (not shown here); white dots indicate input data. In (f) only the axial curves (pink) and ridge curves (blue) of the shock scaffold in (e) are retained.

3D Shape Representation via the Shock Scaffold, F. Leymarie, Ph.D. Thesis 2003, Brown University

Computer Aided Design

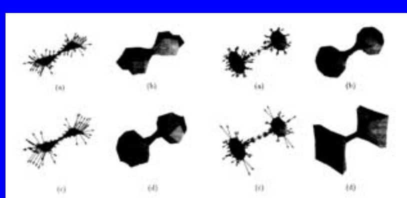

Skeleton-based modeling operations on solids
Duane W. Storti, George M. Turkiyyah, Mark A. Ganter, Chek T. Lim, Derek M. Stal,
ACM Symposium on Solid Modeling and Applications, May 1997.
A skeletal based solid editor, R. Blanding, C. Brooking, M. Ganter, D. Storti, ACM Symposium on Solid Modeling and Aplications, 1999.

Geodesic skeletons for Hexahedral Mesh Generation

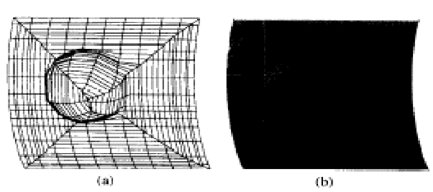

Figure 3: Generation of geodesic line skeletons.

http://www.andrew.cmu.edu/user/sowen/topics/medial.html

Medial surface methods involve an initial decomposition of the volume. As a direct extension of the medial axis method for quad meshing, the domain is subdivided by a set of medial surfaces, which can be thought of as the surfaces generated from the midpoint of a maximal sphere as it is rolled through the volume. The decomposition of the volume by medial surfaces is said to generate map meshable regions. A series of templates for the expected topology of the regions formed by the medial surfaces are utilized to fill the volume with hexahedra. Linear programming is used to ensure element divisions match from one region to another. This method, while proving useful for some geometry, has been less than reliable for general geometry. Robustness issues in generating the medial surfaces as well as providing for all cases of regions defined by the medial surfaces has proved to be a difficult problem. Medial surface methods are incorporated into the FEGS' CADFix [71] hexahedral mesh generator and within Solidpoint's Turbomesh [72] software.

Mesh Decomposition:

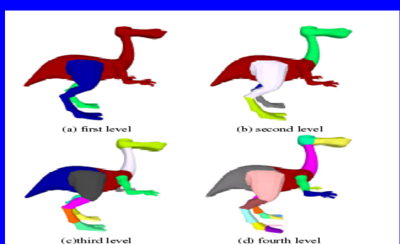

Figure 7: Hierarchical k-way decomposition of a dino-pet

Hierarchical Mesh Decomposition using Fuzzy Clustering and Cuts
By Tal and Katz, Siggraph 2003.

Mirela Tanase, Remco C. Veltkamp: Polygon decomposition based on the straight line skeleton. Symposium on Computational Geometry 2003: 58-67 --- 2D decomposition

Mesh Decomposition

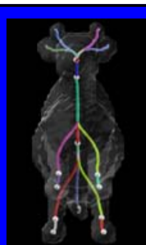

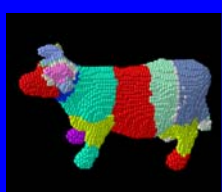

Skeletal Extraction:

- Approximate/simplified shape
- Data Reduction
- Data Comparison
- Data Registration
- Automatic path navigation
- Collision Detection
- Animation
- Morphing
- Alternate Visualization

Scientific Uses

Computer Graphics Uses

Skeleton Construction

Skeleton Construction

- Many algorithms, both for medial surface construction and curve-skeleton/centerline construction
- Many domains, computer graphics & visualization, computational geometry, medical imaging, CAD, artificial intelligence, chemistry/biological sciences.

Broad Categories

- Voronoi Based
- Thinning Based
- Distance Transform Based
- Grassfire Based

Topological Thinning

Skeleton of an S-shaped volume

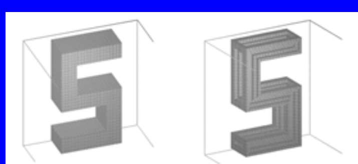

Original Bertrand's method

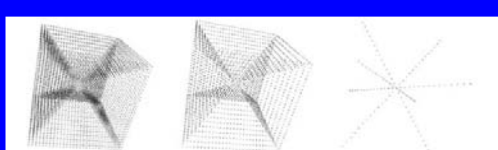

Distance Transform

- Use boundary peeling
- Octree representation
- 2 passes
  - Pass 1: Compute boundary voxels
  - Pass 2: Compute neighbors of boundary voxels, propagate boundary inwards.

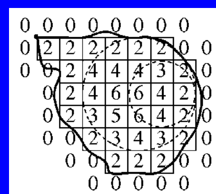

Algorithmic Approaches -- Functional

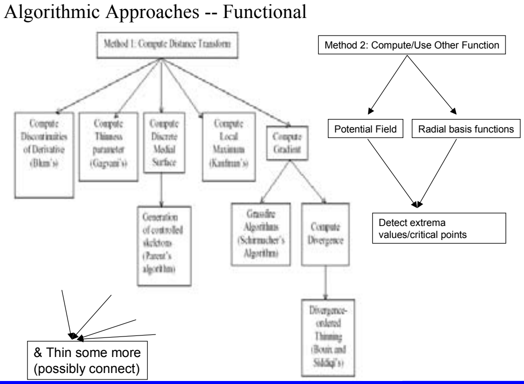

Skeleton Generation : Previous Work

- Voronoi Methods
  - Proximity based subdivision of space.
  - Medial axis is a subset of the VD of boundary points.
  - Have to prune the VD; ensure topological correctness.
- Summary
  - Boundary data; not directly useful for volumes.
  - VD algorithms have numerical limitations.
  - VD algorithms are O(n lg n)
  - Good for regular polyhedral shapes.

Algorithmic Approaches --- Geometric Based

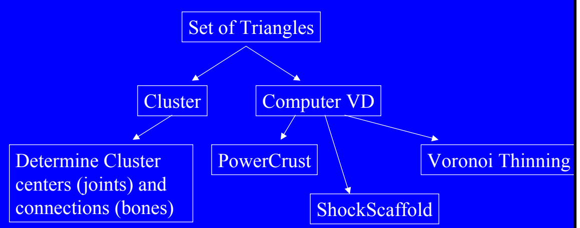

Algorithmic Approaches --- Discrete

- Thin based upon discrete topology (Svennson et. al.)
- 2D slices + combine

Overview of Approaches

- Thinning & Grassfire
- Discrete
- Voronoi & Geometric

Thinning & Grassfire

Parameter Controlled Skeletonization

- Based on the distance transform
- Multi-resolution
  - Density of skeleton is controlled by a thinness parameter
- Reconstructible
- Centered
- *Unconnected but can connect in a postprocessing step*

Thinning & Grassfire

Parameter-Controlled Skeletonization

- Compute the Distance Transform DT_p of every voxel p.
  - Various distance metrics : <3,4,5> or Euclidean
- Compute the mean distance transform MNT_p for 26-neighbors of each voxel p.
- Compute $DT_p - MNT_p$.
- If $DT_p - MNT_p > TP$, add voxel p to the skeleton.

Thinning & Grassfire

Parameter-Controlled Skeleton

"Parameter Controlled Volume Thinning", N. Gagvani and D. Silver. GMIP, V. 61, N 3, 1999.

- Controls the density based on a single Thinness Parameter (TP).
- Higher TP implies thinner skeleton.

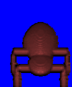

64^3 bug dataset

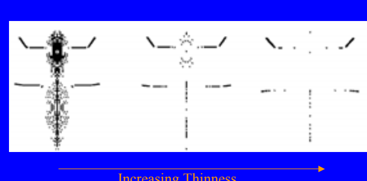

Thinning & Grassfire

Parameter-Controlled

Visible Man Dataset (NLM)

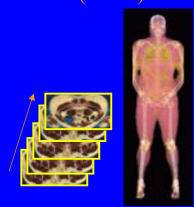

- Keep voxels depending upon their importance for shape description.
- Allows thinned volumes of varying density

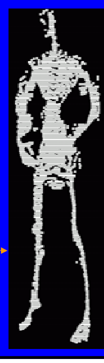

Thinning & Grassfire

Skeleton
--front view

Visible Male Dataset Skeleton

Skeleton
--side view

Need joint information-----

Thinning & Grassfire

Connecting The Skeleton

- Use TP so a dense skeleton results
  - too many skeletal voxels
- Use automatic algorithm-*"skeleton-tree algorithm"*
  - Automatic connectivity
  - Good for animation of amorphous shapes
- Have user define a connectivity --> Articulated skeleton
  - Manual connectivity
  - Good for precise humanoid animation

Thinning & Grassfire

Skeleton-Tree : Summary

- Connects skeletal points into a tree (no cycles).
- Abstract data structure for volumetric operations.
- Encapsulates connectivity information.

Different values for EW will result in different connectivities
$EW_{v1,v2}=\alpha * DIST_{v1,v2}+(1-\alpha) * \|DT_{v1}-DT_{v2}\|, \ \alpha=[0,1].$

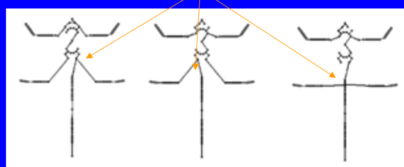

Thinning & Grassfire

Skeleton-tree

Visible Man Dataset

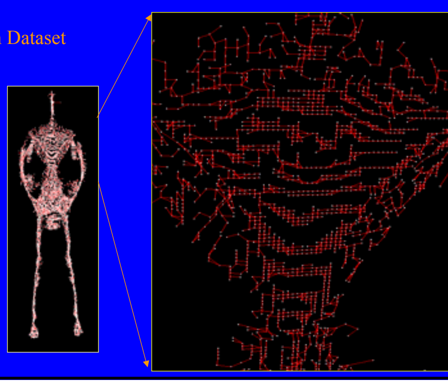

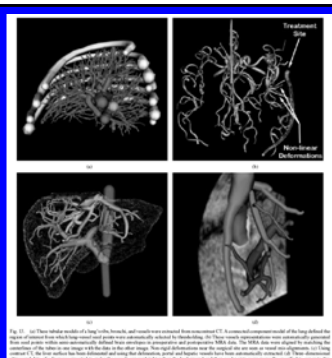

S.R. Aylward and E. Bullit, ***Initialization, Noise, Singularities, and Scale in Height Ridge Traversal for Tubular Object Centerline Extraction.*** 2002

Thinning & Grassfire

Algorithm 1 The divergence-ordered thinning algorithm.

```
Part I: Total Outward Flux
Compute the distance transform of the object D.
Compute the gradient vector field ∇D.
Compute the net outward flux of ∇D using Eq. 5
  For each point P in the interior of the object
    Flux(P) = Σ_{i=1}^{n} < N_i, ∇D(P_i) >,
    where P_i is a 26-neighbor of P and N_i is the outward
    normal at P_i of the unit sphere in 3D, centered at P.
Part II: Homotopy Preserving Thinning
For each point P on the boundary of the object
if (P is simple)
  insert(P, Heap) with Flux(P)
  as the sorting key for insertion
While (Heap.size > 0)
P = HeapExtractMax(Heap)
  if (P is simple)
    if (P is not an endpoint) or (Flux(P) > Thresh)
      Remove P
      for all neighbors Q of P
        if (Q is simple)
          insert(Q, Heap)
    else mark P as a skeletal (end) point
    end { if }
  end { if }
end { while }
```

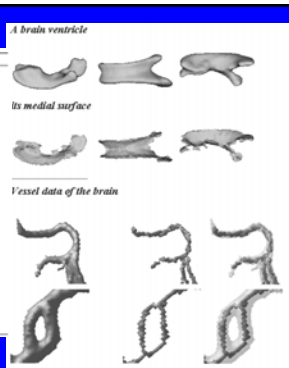

S. Bouix and K. Siddiqui, ***Divergence-Based Medial Surfaces***, European Conf. Computer Vision (Dublin, Ireland), June, 2000.

Thinning & Grassfire

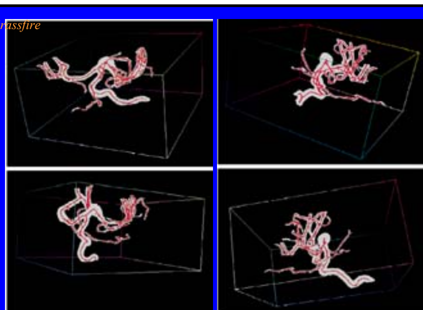

Fig. 6. The shape and reliable path of a blood vessel, shown from four different angles.

T. He, L. Hong, D. Chen and Z. Liang, ***Reliable Path for Virtual Endoscopy: Ensuring Complete Examination of Human Organs***, IEEE Trans. Visualization and Computer Graphics, vol-7, no. 4, pp. 333-342, 2001.

Thinning & Grassfire

1. Reconstruct volume V from 2D slices;
2. Classify V into: external E, internal I, surface B;
3. Perform Euclidean distance transform on I;
4. Initialize L with all the local maximum voxels;
   Sort L in the order of decreasing distance values;
5. $P = \emptyset; U = B$;
   Repeat until $L == \emptyset$
     $v = L.head; L = L - v$; get visible set T_v for v;
     if $(T_v \cap U \neq \emptyset)$
       $P = P \cup \{v\}; U = U - T_v$;
6. Connect P into $C \subset I$ using the shortest path algorithm;
7. $P' = C - P; U = U - \bigcup_{v \in P'} T_v; P = \emptyset$;
8. Repeat until $U == \emptyset$
     select $v \in U$; get $K \subset I$ that is visible from v;
     select $v' \in K$ with the highest distance value;
     $P = P \cup \{v'\}; U = U - T_{v'}$;
9. Connect $C \cup P$ into $C \subset I$ using the shortest path algorithm;
10. Output C.

The pseudocode of the reliable path generation algorithm.

T. He, L. Hong, D. Chen and Z. Liang, ***Reliable Path for Virtual Endoscopy: Ensuring Complete Examination of Human Organs***, IEEE Trans. Visualization and Computer Graphics, vol-7, no. 4, pp. 333-342, 2001.

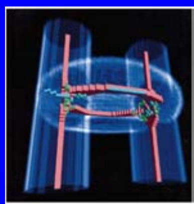

Y. Zhou, A. Kaufman and A.W Toga, ***Three-dimensional Skeleton and Centerline Generation Based on an Approximate Minimum Distance Field***, The Visual Computer, vol. 14, pp. 303-314, 1998.

1. Minimum distance approximation
2. Cluster generation
3. Cluster connection.

We propose an algorithm for generating 18-connected skeletons and centerlines of 3D binary volume data sets. With of an approximate minimum distance field, we express skeletons as a set of clusters with a set of local maximum paths (LMpaths). Each cluster consists of geometrically adjacent voxels with the same local maximum value. Distinct clusters are connected by all possible LMpaths formed by local maximum voxels snaking along, at most, three fixed directions until they meet other clusters. As a 3D extension, we discuss an LMpath traveling on a straight line before and after reaching a saddle point. We generate the shortest centerline connecting two given points with another similar minimum field over skeletal point sets. The results generated by the algorithms on an experimental data set and colon CT and brain MRI data sets demonstrate their efficiency.

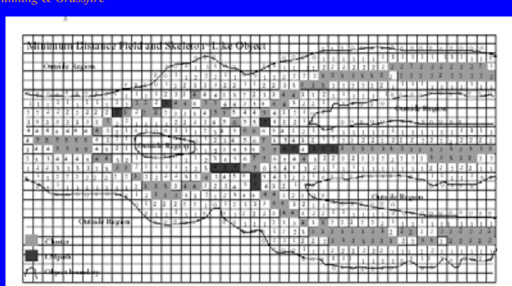

Thinning & Grassfire

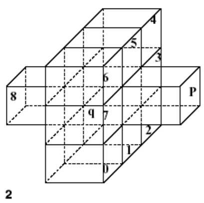

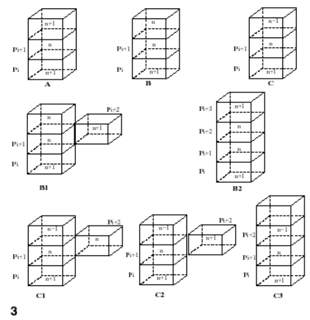

Fig. 1. Minimum distance field and skeleton-like object

Fig. 2. Relationship between indirect F-neighbor and F-neighbor: voxel 8 is an indirect F-neighbor of voxel *q* relative to voxel *p*; voxels 1, 3, 5 and 7 are direct F-neighbors of *q* relative to *p*; voxels 0, 2, 4 and 6 are indirect E-neighbors of *q* relative to *p*

Fig. 3. The cases for path generation

Thinning & Grassfire

K. PALAGYI, A. KUBA, *Directional 3D Thinning using 8 Subiterations*, Proc. DGCI '99, LNCS 1568, pp. 325–226, Springer, 1999.

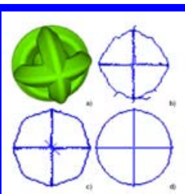

Figure 4: *Three-rings object (a). Centerlines: PK thinning method (b), VKG thinning method (see also Sec. 4) (c), our method (d)*

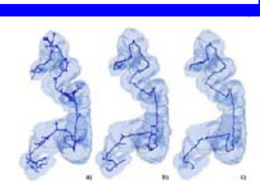

Figure 11: *Colon centerline: VKG method (a), our method $R_0 = 0$ (b) and $R_0 = 15$ (c)*

A. MANZANERA, T. BERNARD, F. PRETEUX, B. LONGUET, *Medial faces from a concise 3D thining algorithm*, Proc. ICCV '99, pp. 337–343, IEEE CS Press, 1999.

Automated generation of control skeletons for use in animation. L. Wade and R. Parent, The Visual Computer, March 2002

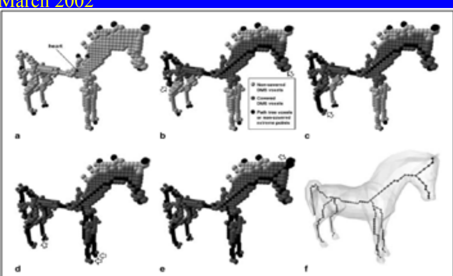

Fig. 3a–f. Forming path-tree extension. **a** DMS of a horse with the heart voxel labeled and the extreme points drawn as *black spheres*. The extreme point at the tip of the tail is the first point of the path tree. **b** The first extension to the path tree reaches from the tail to the nose. **c** The second extension reaches to the right hind hoof. **d** The next three extensions branch out to the other hooves. **e** The final branch extends to the ears. The remaining extreme points are not far enough from the covered region to warrant further extensions of the path tree. **f** The completed path tree without the other DMS voxels; path-tree voxels are drawn as *small spheres* to allow the edges of the path tree to be seen

Here you can see the intermediate results of the shrinking process for a 3D ``carrot'' shape:

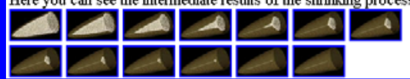

Algorithm:

- compute boundary surface
- compute distance map gradient
- move vertices along gradient
- constraints prevent neighbours from moving too far apart
- stop where gradient vanishes
- simplify degenerated surface by clustering nearby vertices/edges

Some more images:

H. Schirmacher, M.Zockler, D. Stalling and H. Hege, ***Boundary Surface Shrinking – A Continuous Approach to 3D Center Line Extraction***, Proc. Image and Multidimensional Digital Signal Processing, Alpbach, pp. 25-28, 1998.

The following are the steps required to find the skeleton of a planar object:

1. Compute the potential distribution $V = v(x, y)$ inside the object,
2. Compute the electrostatic field in x and y directions: E_x and E_y, respectively,
3. Find the equipotential contour at a given potential v_{con},
4. Detect significant convexities and concavities along an equipotential contour, and
5. Trace skeletal points starting from points of significant convexities and concavities.

T. Grigorishin and Y.H. Yang, ***Skeletonization: An Electrostatic Field-Based Approach***, vol. 1, pp. 163-177, 1998.

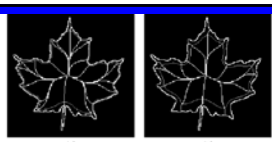

(a) (b)

Figure 6: The multiscale capability of the proposed approach. Skeletons generated for a maple leaf at two different starting equipotentials: (a) 90, and (b) 60.

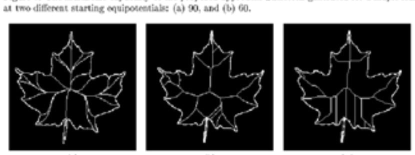

(a) (b) (c)

Figure 7: Skeletons generated for the image of a maple leaf. (a) EFT-based approach. Skeleton started at the equipotential contour 80; (b) DT-based algorithm; (c) Charge Particle Method.

T. Grigorishin and Y.H. Yang, ***Skeletonization: An Electrostatic Field-Based Approach***, vol. 1, pp. 163-177, 1998.

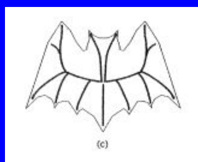

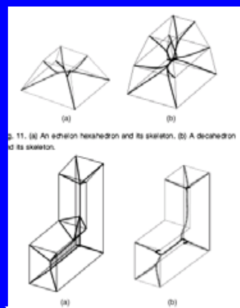

N. Ahuja and J. Chuang. ***Shape Representation Using a Generalized Potential Field Model***, IEEE Trans. Pattern Analysis and Machine Intelligence, vol119. 1997

Chuang et. al, Skeletonization of 3D Object using generalized Potential Field, 22(11) November 2000.

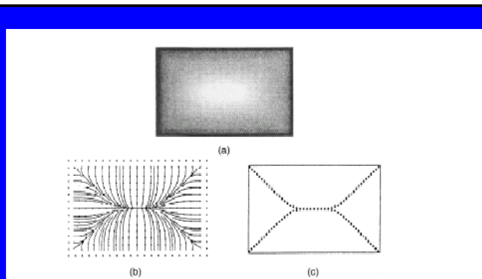

Algorithm MAT_Generalized_Polyhedron

- Step 1: Follow the direction of the force to traverse the skeleton (potential valley) until a zero force is obtained, i.e., a potential minimum is reached.
- Step 2: Repeat Step 1 for each of the seed points.
- Step 3: End the skeleton computation if there is only one potential minimum.
- Step 4: Derive additional skeleton branches by identifying potential valleys connecting neighboring potential minima.

$$\int_S \frac{dS}{R^m}, \qquad m \geq 2,$$

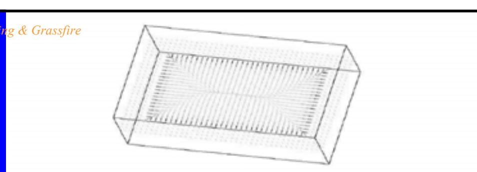

Figure 1: *Force vectors formed from the block object of size* 19 × 29 × 41

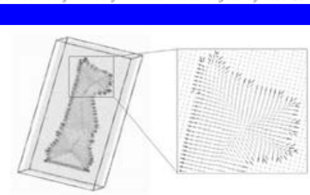

Figure 2: *Force vectors formed from the chess piece knight of size* 52 × 100 × 52

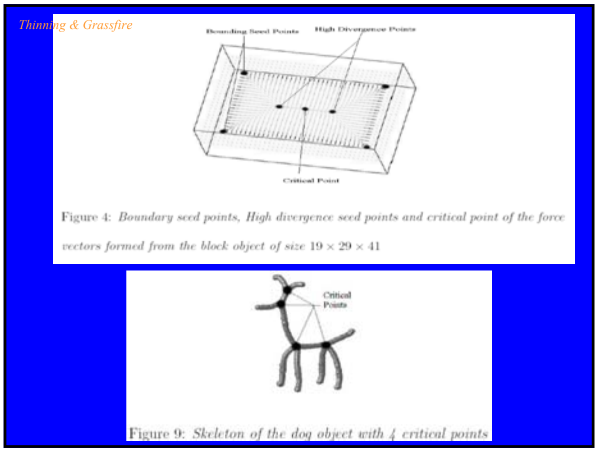
Thinning & Grassfire
Bounding Seed Points
High Divergence Points
Critical Point
Figure 4: Boundary seed points, High divergence seed points and critical point of the force vectors formed from the block object of size 19 × 29 × 41
Critical Points
Figure 9: Skeleton of the dog object with 4 critical points

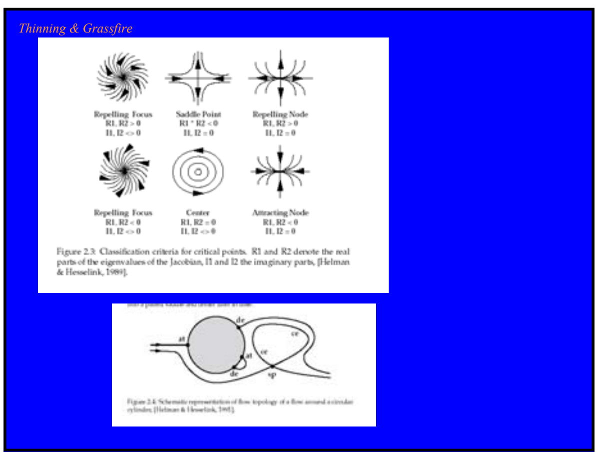
Thinning & Grassfire
Repelling Focus
R1, R2 > 0
I1, I2 <> 0
Saddle Point
R1 * R2 < 0
I1, I2 = 0
Repelling Node
R1, R2 > 0
I1, I2 = 0
Repelling Focus
R1, R2 < 0
I1, I2 <> 0
Center
R1, R2 = 0
I1, I2 <> 0
Attracting Node
R1, R2 < 0
I1, I2 = 0
Figure 2.3 Classification criteria for critical points. R1 and R2 denote the real parts of the eigenvalues of the Jacobian, I1 and I2 the imaginary parts, [Helman & Hesselink, 1989].

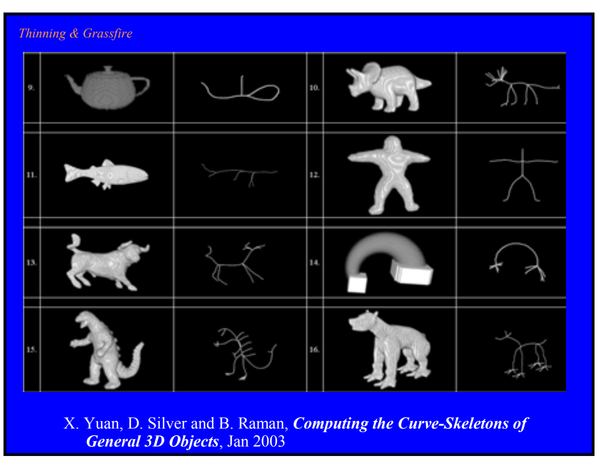
Thinning & Grassfire
X. Yuan, D. Silver and B. Raman, Computing the Curve-Skeletons of General 3D Objects, Jan 2003

Geometric Based Algorithms

Voronoi

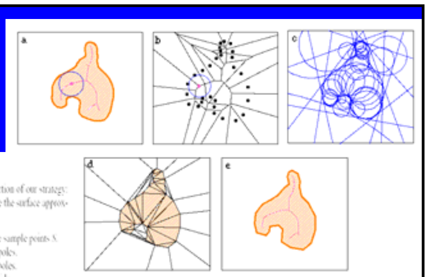

5 Algorithm

The basic algorithm is a straightforward reflection of our strategy: first estimate the MAT, and then use it to define the surface approximation.

1. Compute the Voronoi diagram of the sample points S.
2. For each sample point, compute its poles.
3. Compute the power diagram of the poles.
4. Label each pole either inside or outside.
5. Output the power diagram faces separating the cells of inside and outside poles as the power crust.
6. Output the regular triangulation faces connecting inside poles as the power shape.

N. Amenta, S. Choi and R. K. Kolluri, ***The Power Crust***, Proc. Of 6th ACM Symposium on Solid Modeling, pp. 249-260, 2001

Voronoi

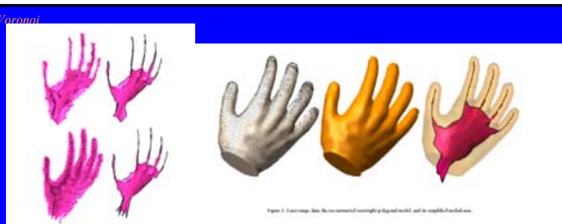

Figure 16. Above, the power shape of the original hand model and its simplification with 352,985 and 7805 faces respectively. Below, the power shape of the hand model with added Gaussian noise and its simplification, with 438,855 and 7003 faces respectively. Notice that the two simplified models are very similar; this is because the simplification procedure removes unstable features which might be due to small surface perturbations.

Voronoi

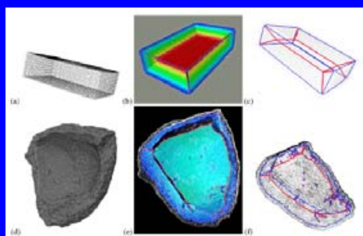

Figure 1.4: The shock scaffold of a rectangular box sampled by 7326 points (a) is depicted in (b) and (c). The flow along sheets is shown using the color spectrum, where blue means close to the boundary, and red means as far as possible. In (c) the geometry for the interior of the shock sheets is left implicit, and axial curves at the intercepts of shock sheets are shown in pink, while ridge curves at the boundaries of shock sheets are shown in blue. This synthetic example serves as a prototype of many real shapes, such as the pot sherd in (d) which can be thought of as a deformed rectangular box with additional surface perturbations (approximatively 40 000 point samples here). The shock scaffold of this sherd is shown in (e) with the flow along sheets color-coded similarly to (b) where the missing colors of the spectrum correspond to the symmetries away from the concave part of the pot sherd (not shown here); white dots indicate input data. In (f) only the axial curves (pink) and ridge curves (blue) of the shock scaffold in (e) are retained.

3D Shape Representation via the Shock Scaffold, F. Leymarie, Ph.D. Thesis 2003, Brown University

Geometric

Hierarchical Mesh Decomposition using Fuzzy Clustering and Cuts
By Tal and Katz, Siggraph 2003.

1. Assigning distances to all pairs of faces in the mesh.
2. After computing an initial decomposition, assigning each face a probability of belonging to each patch.
3. Computing a fuzzy decomposition by refining the probability values using an iterative clustering scheme.
4. Constructing the exact boundaries between the components, thus transforming the fuzzy decomposition into the final one.

Once the hierarchical k-way decomposition is computed, the decomposition tree is traversed and a tree of joints is generated. At each level of the hierarchy, joints between the central patch and its adjacent patches are created. Each joint is positioned at the center

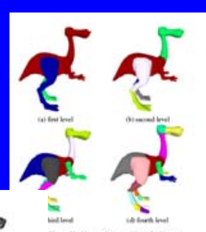

Hierarchical k-way decomposition of a dino-pet

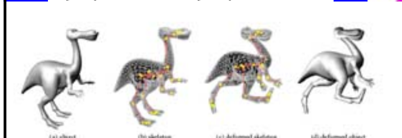

Figure 2: Deformation of a dino-pet

Discrete Based

Discrete

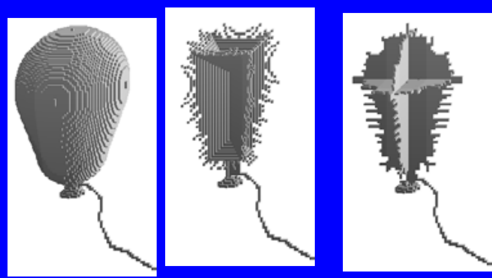

S. Svennson, I. Nystrom and G. Sanniti di Baja, ***Curve Skeletonization of Surface-like Objects in 3D Images Guided by Voxel Classification***, Pattern Recognition Letters, pp. 1419-1426, 2002.

Discrete

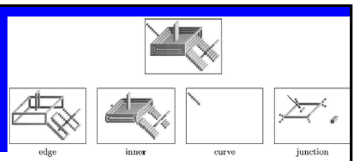

Fig. 1. A surface-like object, top, with its classification, bottom.

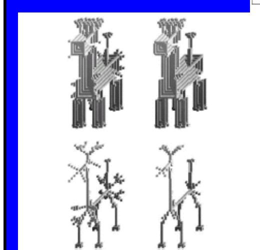

Fig. 5. Surface-like object before and after simplification, top. The corresponding curve skeletons, bottom.

Discrete

A. Telea and A. Vilanova, ***A Robust Level-Set Algorithm for Centerline Extraction***, Eurographics-IEEE TCVG Symp. On Visualization, 2003.

Discrete

A. Telea, A. Vilanova / Level Set Centerlines

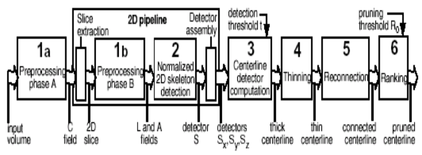

Figure 2: *Centerline extraction pipeline*

Comparison Between Methods

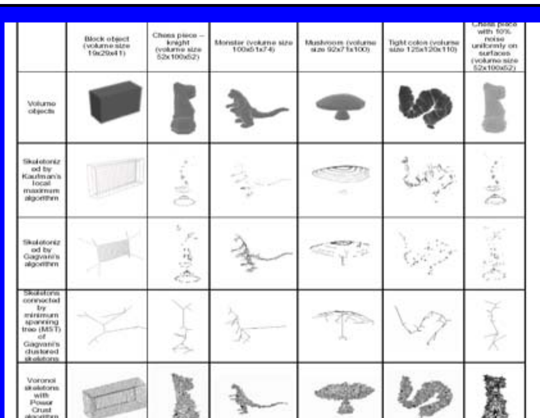

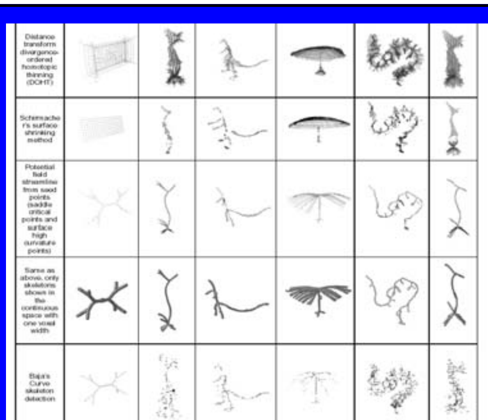

Summary

- Many applications
- Many different methods

Acknowledgements

- DOE
- NSF
- Brooks
- CAIP Center

VIZLAB

Laboratory for Visiometrics and Modeling

http://www.caip.rutgers.edu/vizlab.html